

# Characterization of $^{64}\text{Cu}$ -DOTA-Conatumumab: A PET Tracer for In Vivo Imaging of Death Receptor 5

Raffaella Rossin<sup>1</sup>, Tadahiko Kohno<sup>2</sup>, Aviv Hagooly<sup>1</sup>, Terry Sharp<sup>1</sup>, Brian Gliniak<sup>2</sup>, Thomas Arroll<sup>3</sup>, Qing Chen<sup>2</sup>, Art Hewig<sup>3</sup>, Paula Kaplan-Lefko<sup>2</sup>, Greg Friberg<sup>2</sup>, Robert Radinsky<sup>2</sup>, Jeffrey L. Evelhoch<sup>2</sup>, Michael J. Welch<sup>1</sup>, and Dah-Ren Hwang<sup>2</sup>

<sup>1</sup>The Edward Mallinckrodt Institute of Radiology, Washington University, St. Louis, Missouri; <sup>2</sup>Amgen Inc., Thousand Oaks, California; and <sup>3</sup>Amgen Inc., Seattle, Washington

Conatumumab is a fully human monoclonal antibody that binds to and activates human death receptor 5 (DR5; also known as TRAIL receptor 2). The purpose of this study was to characterize  $^{64}\text{Cu}$ -labeled conatumumab as a PET tracer for imaging DR5 in tumors. **Methods:** DOTA-conatumumab was synthesized by incubating conatumumab with 2,2',2''-(10-(2-(2,5-dioxypyrrolidin-1-yloxy)-2-oxoethyl)-1,4,7,10-tetraazacyclododecane-1,4,7-triyl) triacetic acid (DOTA-NHS). The absolute numbers of DOTA molecules per conatumumab molecules were determined by matrix-assisted laser desorption ionization mass spectrometry and electrospray ionization quadrupole time-of-flight mass spectrometry.  $^{64}\text{Cu}$ -DOTA-conatumumab was prepared by incubating  $^{64}\text{CuCl}_2$  (33–222 MBq) with DOTA-conatumumab at 37°C for 1 h. Binding of conatumumab and DOTA-conatumumab to Fc-coupled human DR5 (huTR2-Fc) was tested in a kinetic analysis assay, and the biologic activity of copper-DOTA-conatumumab was measured using a caspase-3/7 luminescent assay. In vivo evaluation of DOTA-conatumumab and copper-DOTA-conatumumab was done in severe combined immunodeficiency mice bearing Colo205 xenografts: tissue uptake was determined with biodistribution studies, and small-animal PET and autoradiography were used to determine the uptake of  $^{64}\text{Cu}$ -DOTA conatumumab into tumors and other tissues. **Results:** DOTA-conatumumab was prepared with an average of 5 DOTA molecules per conatumumab molecule. The in vitro median effective concentration required to induce a 50% effect of DOTA-conatumumab and conatumumab from the assay were 389 and 320 pM, respectively. The median effective dose ( $\pm$ SD) of DOTA-conatumumab and conatumumab via the caspase assay was  $135 \pm 31$  and  $128 \pm 30$  pM, respectively. In female CB17 severe combined immunodeficiency mice bearing Colo205 xenografts, DOTA-conatumumab and conatumumab inhibited tumor growth to the same extent. Small-animal PET studies showed tumor uptake at 24 h after injection of the tracer, with a mean standardized uptake value of 3.16 ( $n = 2$ ). Tumor uptake was decreased by the coadministration of 400  $\mu\text{g}$  of unlabeled conatumumab (mean standardized uptake value, 1.55;  $n = 2$ ), suggesting saturable uptake. Tissue uptake determined by biodistribution studies was in agreement with the small-animal PET findings. **Conclusion:**

These results suggest that  $^{64}\text{Cu}$ -DOTA-conatumumab is a potential PET tracer for imaging DR5 in tumors and may be useful for measuring on-target occupancy by conatumumab.

**Key Words:** conatumumab; death receptor 5; PET; tracer;  $^{64}\text{Cu}$

**J Nucl Med 2011; 52:942–949**

DOI: 10.2967/jnumed.110.086157

**T**umor necrosis factor-related apoptosis-inducing ligand (TRAIL) is a member of the tumor necrosis factor superfamily of cytokines that selectively induces apoptosis in cancer cells. TRAIL binds specifically to 4 cell-surface receptors (death receptor 4 [DR4] and 5 [DR5] and decoy receptors 1 and 2) and a soluble receptor (osteoprotegerin) (1–4). Among the 4 surface receptors, only DR4 and DR5 are capable of transducing apoptotic signals. The other 3 receptors lack the cytoplasmic death domain and are referred to as decoy receptors. After stimulation by TRAIL ligand, the death receptors aggregate at the cell surface and activate a caspase cascade, which results in cell death. The use of proapoptotic receptor agonists to treat cancer is an area of active drug research (5).

Conatumumab is a fully human monoclonal antibody that mimics endogenous TRAIL and acts as a human DR5 agonist antibody. Binding of conatumumab to DR5 induces apoptosis in transformed human tumor cell lines in vitro and inhibits the growth of human xenograft tumors in mice (6). In the first-in-human trial of conatumumab in cancer patients with advanced solid tumors, a partial response was observed in a patient with non-small cell lung cancer (7). Currently, conatumumab is being evaluated in numerous phase 2 trials across several oncology indications (8).

It would be of great interest to identify DR5-positive tumors with a noninvasive imaging probe and to inform clinical dose selection by measuring tumor DR5 receptor occupancy by conatumumab in cancer patients. Recently, the  $^{99\text{m}}\text{Tc}$ - and  $^{68}\text{Ga}$ -labeled DR4- and DR5-specific antibodies, HGS-ETR1 and HGS-ETR2, respectively, have been used successfully to detect upregulation of DR4 and

Received Dec. 20, 2010; revision accepted Feb. 28, 2011.

For correspondence or reprints contact: Dah-Ren Hwang, Amgen Inc., One Amgen Center Dr., Thousand Oaks, CA 91320-1799.

E-mail: dahh@amgen.com

COPYRIGHT © 2011 by the Society of Nuclear Medicine, Inc.

DR5 by paclitaxel in vivo (9). A specific tracer for imaging DR5-positive tumors would be of potential value to the clinical development of conatumumab.

This report describes the synthesis and characterization of DOTA-conatumumab and  $^{64}\text{Cu}$ -DOTA-conatumumab.  $^{64}\text{Cu}$  has a convenient half-life of 12.7 h and has been widely used for labeling antibodies for PET (10,11). The potential utility of  $^{64}\text{Cu}$ -DOTA-conatumumab as a tracer to image DR5-positive tumors is presented. In addition, the saturability of tracer uptake was examined to evaluate its potential for measuring tumor DR5 receptor occupancy by conatumumab.

## MATERIALS AND METHODS

### Animals

All animal experiments were conducted in compliance with the Guidelines for the Care and Use of Research Animals established by Washington University Medical School's Animal Studies Committee. Female CB17 severe combined immunodeficiency (SCID) mice (age, 6–8 wk; weight,  $18.0 \pm 1.03$  g) were obtained from Charles River Laboratories. Tumor volumes ( $V$ ,  $\text{mm}^3$ ) were calculated using the ellipsoid formula  $V = 1/2 \times A \times B^2$ , where  $A$  is the diameter of the long axis (mm) and  $B$  is the short axis (mm) measured with calipers (12,13).

### Chemistry

**DOTA-Conatumumab.** A solution of conatumumab (0.5 mL of a stock solution of 30 mg/mL in phosphate-buffered saline [PBS], equivalent to 15 mg or 0.1  $\mu\text{mol}$ ) was adjusted to pH 8.5 with 2.5  $\mu\text{L}$  of 1 M sodium bicarbonate. To the solution was added 1.14 mg of 2,2',2''-(10-(2-(2,5-dioxopyrrolidin-1-yl)oxy)-2-oxoethyl)-1,4,7,10-tetraazacyclododecane-1,4,7-triyl)triacetic acid (DOTA-NHS; 22.8  $\mu\text{L}$  of a solution [50 mg/mL] in dimethyl sulfoxide). The mixture was incubated at room temperature for 2 h and purified using a NAP10 desalting column (GE Healthcare). DOTA-conatumumab was eluted with 10 mM sodium acetate (pH 5.2) in 5% sucrose, and the product fractions were pooled. The final protein concentration (4.8 mg/mL) was determined with an 8453 UV-Visible Spectrophotometer (Agilent Technologies) at 280 nm. Purity was determined by size-exclusion (SE) high-pressure liquid chromatography and was greater than 98%. Matrix-assisted laser desorption ionization mass spectrometry (MALDI-MS) and electrospray ionization quadrupole time-of-flight MS (ESI-QTOF-MS) were used to characterize DOTA-conatumumab and to determine the absolute numbers of DOTA molecules per conatumumab molecules. For the ESI-QTOF-MS analysis, DOTA-conatumumab samples were pretreated with an amidase (PNGaseF) to remove oligosaccharides from the glycoprotein. MALDI-MS and ESI-QTOF were performed on a MALDI micro MX system (Waters) and a Q-TOF Premier Mass spectrometry system (Waters), respectively. Isoelectric focusing gel electrophoresis analysis was performed to determine the efficiency of the DOTA-conatumumab coupling reaction using a NOVEX PowerEase 500 power supply, an Xcell Surelock minicell, and the NOVEX Pre-Cast IEF Gel, pH 3–10 (Invitrogen).

**Copper-DOTA-Conatumumab.** DOTA-conatumumab (7.8 mg, 52 nmol) and  $\text{CuCl}_2$  (18.5 mg) in 20 mL of ammonium acetate buffer (0.2 mM, pH 5.5) were incubated at 43°C for 90 min. Unreacted  $\text{CuCl}_2$  was removed by dialysis in a sodium acetate buffer (10 mM in 9% sucrose, pH 5.0) at 4°C for 24 h using a Slide-A-Lyzer 2K cartridge (Pierce Biotechnology, Inc.). The final protein concentration was 4.03 mg/mL.

$^{64}\text{CuCl}_2$  was generated on a CS-15 cyclotron (Washington University Medical School) via the  $^{64}\text{Ni}(p,n)^{64}\text{Cu}$  nuclear reaction, as previously reported (10).  $^{64}\text{Cu}$ -DOTA-conatumumab was prepared by incubating  $^{64}\text{CuCl}_2$  (33–222 MBq) in 0.5 M HCl (1–6  $\mu\text{L}$ ) with DOTA-conatumumab (100–200  $\mu\text{g}$ , 200  $\mu\text{L}$  of 0.1 M ammonium acetate, pH 5.5) at 37°C for 1 h. To remove unbound  $^{64}\text{Cu}^{2+}$ , 5  $\mu\text{L}$  of an ethylenediaminetetraacetic acid (EDTA; 10 mM) solution were added. After incubation at room temperature for 10 min, the reaction mixture was purified using a desalting spin column (2 mL; Pierce), and  $^{64}\text{Cu}$ -DOTA-conatumumab was eluted in PBS.

The radiochemical purity was greater than 95%, as determined by radio-thin-layer chromatography (radio-TLC) and SE fast protein liquid chromatography (SE FPLC). Radio-TLC conditions were as follows: instant thin-layer chromatography silica gel plates (Pall Life Sciences) and a 1:1 solvent mixture of aqueous 10% ammonium acetate (w/v) and methanol. TLC plates were scanned using an AR-200 radio-TLC scanner (Bioscan). The  $R_f$  values for  $^{64}\text{Cu}$ -DOTA-conatumumab and  $^{64}\text{Cu}$ -EDTA were 0.0 and 0.9, respectively. SE FPLC was performed on a Pharmacia/LKB chromatograph with a Superose 12 SE column (GE Healthcare) eluted with a solution of 20 mM *N*-(2-hydroxyethyl)piperazine-*N'*-(2-ethanesulfonic acid) and 150 mM NaCl (pH 7.3) at a flow rate of 0.8 mL/min. The retention times of  $^{64}\text{Cu}$ -DOTA-conatumumab and  $^{64}\text{Cu}$ -EDTA were 17 and 25 min, respectively.

**Isotopic Dilution Assay for DOTA-Conatumumab.** The average number of accessible DOTA for chelating copper was determined by isotopic dilution (14). Four solutions of copper (II) chloride were prepared by aliquoting 20, 30, 40, and 60  $\mu\text{L}$  of a 0.21 mM copper (II) chloride solution spiked with  $^{64}\text{CuCl}_2$  into ammonium acetate buffer (0.1 M, pH 5.5) in a total volume of 0.1 mL. To these copper (II) chloride solutions, a solution of 80  $\mu\text{g}$  of DOTA-conatumumab in a 10 mM sodium acetate buffer and 9% sucrose, pH 5.5, was added. The amount of copper (II) chloride was 4.24, 6.36, 8.48, and 12.72 nmol, respectively. After 1 h of incubation at 37°C, 50  $\mu\text{L}$  of a 10 mM EDTA solution in 0.1 M disodium phosphate buffer (pH 7.5) were added to remove any nonbound cupric ions. Each solution aliquot was analyzed by radio-TLC. For each concentration of copper (II), the number ( $N$ ) of effective DOTA chelates attached to the antibodies was determined from the percentage labeling efficiency (obtained from the radio-TLC), and the equivalent of copper was added according to the following equation:  $N = \text{labeling efficiency} \times \text{equivalent of copper (II)}$ .

The numbers of effective DOTA chelates per DOTA-conatumumab from 4 experiments were averaged to determine the average number of DOTA per DOTA-conatumumab that are accessible for copper chelation.

**Stability of  $^{64}\text{Cu}$ -DOTA-Conatumumab.** The in vitro stability of  $^{64}\text{Cu}$ -DOTA-conatumumab was examined after incubation for 1, 6, and 24 h in mouse serum at 37°C. At the end of the incubation period, EDTA was added to trap free  $^{64}\text{Cu}$ . Samples were analyzed by radio-TLC or SE FPLC.

The in vivo stability of  $^{64}\text{Cu}$ -DOTA-conatumumab was examined in female CB17 SCID mice. About 3.7 MBq of the tracer (with  $\sim 4.5$   $\mu\text{g}$  starting DOTA-conatumumab) in 0.1 mL of PBS was injected intravenously into SCID mice. Blood samples were collected at 1, 6, and 24 h after injection and analyzed by radio-TLC and SE FPLC.

### In Vitro Characterization of DOTA-Conatumumab

**Biacore Receptor Binding Inhibition Assay.** The binding affinity of conatumumab and DOTA-conatumumab to Fe-coupled human

DR5 (huTR2-Fc) was determined using a Biacore-based binding assay. A Biacore 3000 instrument from GE Healthcare was used in this study. Conatumumab was immobilized on the second flow cell of a CM5 chip using amine coupling with a density of approximately 8,000 response unit. The first flow cell was used as a background control. HuTR2-Fc (1 nM) was mixed with a serial dilution of conatumumab or DOTA-conatumumab (range, 0.02–40 nM) in PBS plus bovine serum albumin (0.1 mg/mL) and 0.005% surfactant P20 (GE Healthcare). Binding of the free huTR2-Fc in the mixed solutions was measured by injecting over the antibody-coated surface. Baseline huTR2-Fc binding signal to the conatumumab surface was determined in the absence of added soluble conatumumab (100%). Increasing concentrations of soluble conatumumab or DOTA-conatumumab blocked huTR2-Fc binding to the immobilized conatumumab surface, resulting in decreased huTR2-Fc binding signal. By plotting the huTR2-Fc binding signal versus the conatumumab or DOTA-conatumumab concentrations, we calculated the median effective concentration required to induce a 50% effect using the nonlinear regression curve fit of the Prism 4 software (GraphPad Software Inc.).

**In Vitro Caspase-3/7 Luminescent Assay.** This bioassay was a 96-well plate format luminescent assay that measured the biologic activity of conatumumab by its ability to induce activation of caspase-3/7 as a positive marker for cell death. Colo205 cells ( $2 \times 10^4$ ) were added to wells containing vehicle control test samples (such as reference conatumumab standards), copper-DOTA-conatumumab, or DOTA-conatumumab. The plates were then incubated at 37°C and 5% CO<sub>2</sub> for 2 h before the addition of Caspase-Glo 3/7 Assay reagent (Promega). After development on a shaker for 2 h at room temperature, the plates were read on an EnVision plate reader (PerkinElmer). Data were analyzed by a 5-parameter logistic model for the curve fitting of the full curve with upward slope using StatLIA software (Brendan Technologies Inc.). The median effective dose (ED<sub>50</sub>) and the potency relative to conatumumab (relative potency percent) were obtained.

**In Vivo Evaluation of DOTA-Conatumumab and Copper-DOTA-Conatumumab.** Female CB17 SCID mice were pretreated 1 d before tumor challenge with antiasialo GM1 antibody (Wako Pure Chemical Industries) injected intraperitoneally to deplete natural killer cells. Colo205 cells ( $1 \times 10^6$ ) were implanted subcutaneously in the mid-thoracic region of the mice (6). Although the mid-thoracic region is not ideal for small-animal PET studies because of the possibility of spillover effects, for consistency we chose the same Colo205 xenograft model that was used in previous conatumumab characterization studies. Treatment began on day 13, when tumors were established ( $\sim 350$  mm<sup>3</sup>).

Conatumumab, DOTA-conatumumab, and copper-DOTA-conatumumab were administered by intraperitoneal injection at doses of 0.25, 2.5, or 25 µg/d/mouse on days 13, 15, and 17. A vehicle control group (10 mM sodium acetate, 9% sucrose, 0.04% polysorbate 20, pH 5.2) and an IgG1 isotype control group were also included. Tumor volumes were determined twice weekly with calipers.

### Biodistribution Studies

Biodistribution studies were performed on female SCID mice bearing Colo205 tumors (16 d after tumor cell implant). All animals were administered approximately 0.33 MBq of <sup>64</sup>Cu-DOTA-conatumumab (8-µg mass) intravenously. Animals were divided into groups ( $n = 4$  per group). Competitive blocking was obtained by coinjecting 400 µg of conatumumab (50-fold excess). At

predetermined time points, animals were sacrificed. Selected organs and tissues were removed, blotted dry, weighed, and counted in an automatic well counter. Tissue uptake was expressed as percentage injected dose per gram of tissue (%ID/g).

### Small-Animal PET Studies

Two Focus microPET scanners (Siemens Medical Solutions) were used in this study. Two pairs of SCID mice bearing Colo205 tumors (16 d after implant) were used. Each pair consisted of a control mouse (tracer only) and a blocked mouse (tracer plus a 400-µg conatumumab blocking dose). Each pair was scanned side by side in the same scanner at 1, 6, and 24 h after tracer injection. <sup>64</sup>Cu-DOTA-conatumumab ( $\sim 3.7$  MBq; total mass, 4.5 µg) was administered into the tail vein. The first small-animal PET session consisted of a 0- to 60-min acquisition. The image data were reconstructed into a single frame. Immediate qualitative analysis of the imaging data was performed at the end of the imaging session to ensure the accuracy of the radiopharmaceutical injection. Animals were reimaged (10-min static scans) at 6 and 24 h after radiopharmaceutical injection. For each imaging session, the mice were anesthetized with inhalant isoflurane anesthesia (1.5%–2.0% via a nose cone). After induction of anesthesia, the mice were secured in a supine position and placed in an acrylic imaging tray. They were hemodynamically monitored, and body temperature was maintained as necessary. Fiducial markers were placed on the imaging tray to facilitate PET/CT coregistration. CT was performed on a MicroCAT II (Siemens) scanner for anatomic visualization.

Standardized uptake values (SUVs) of tumor, muscle, heart, kidney, liver, and spleen were determined by measuring regions of interest (ROI) that encompassed the entire organ from the PET images. SUVs were calculated according to the following equation:  $\text{Uptake}_{\text{ROI}} (\text{Bq/mL}) / (\text{dose administered} [\text{Bq}] / \text{animal weight} [\text{g}])$ .

After the last scan session, animals were sacrificed, and biodistribution studies were performed to confirm the small-animal PET findings.

### Autoradiography Studies

A third pair of animals was also injected with the tracer with or without the blocker. The animals were not scanned but sacrificed 24 h after injection, and the tumors were removed for autoradiography studies to confirm the tumor uptake. The tumors were embedded in tissue-freezing medium, snap-frozen, and sectioned into 1-mm slices. Tissue slices were scanned using an Electronic Autoradiography Instant Imager (Packard Instrument Company).

## RESULTS

### Characterization of DOTA-Conatumumab

The molecular weights of conatumumab and DOTA-conatumumab (determined by MALDI-MS) were 148,146 and 150,387 Da, respectively. The average number of DOTA molecules per conatumumab molecules was 5.8, as determined by dividing the mass difference between DOTA-conatumumab (150,387 Da) and conatumumab (148,146 Da) by the molecular weight of DOTA (386 Da).

Each DOTA-coupled conatumumab species was expected to have a unique mass peak, and these mass peaks were clearly resolved by ESI-QTOF-MS as shown in Figure 1. The average molecular weight of DOTA-conatumumab and con-



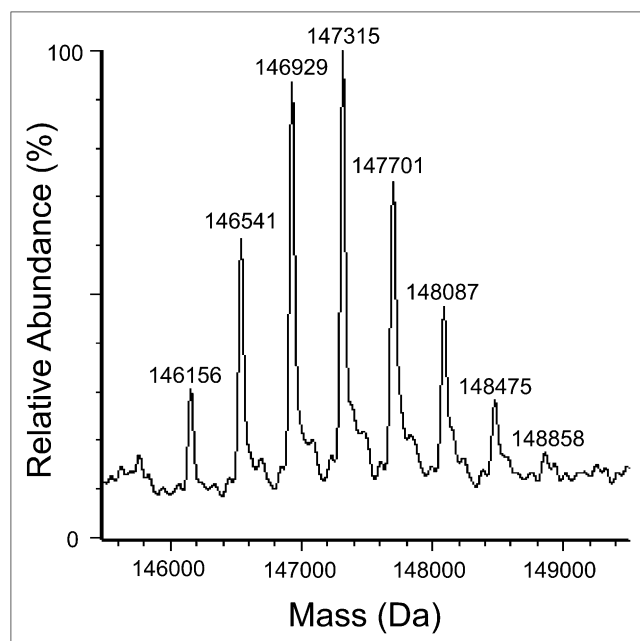


**FIGURE 1.** ESI-QTOF-MS of DOTA-conatumumab.

atumumab using this method was 147,315 Da and 145,395 Da, respectively. The average number of DOTA molecules per conatumumab molecules was determined to be 4.9 [(147,315 Da – 145,395 Da)/386 Da].

The ESI-QTOF-MS method provides a range of the absolute numbers of DOTA per antibody. For comparison, we also performed the isotope dilution method to determine the functional numbers of DOTA per antibody. The average number of DOTA molecules per conatumumab molecules ( $\pm$ SD) was  $3.9 \pm 0.3$ .

To examine the efficiency of the conatumumab DOTA-coupling reaction, isoelectric focusing was performed. Six distinct bands with isoelectric point values between 5.8 and 9.0 were observed. The range of values was due to the introduction of DOTA functional groups to conatumumab. There was no detectable unmodified conatumumab in this analysis.

#### **In Vitro Characterization of DOTA-Conatumumab and Copper-DOTA-Conatumumab**

An in vitro Biacore receptor-binding inhibition assay was used to determine the affinities of conatumumab and DOTA-conatumumab for DR5. The effective concentrations of conatumumab and DOTA-conatumumab that inhibit 50% of DR5 receptor binding ( $EC_{50}$ ) were similar at 320 pM and 389 pM, respectively.

An in vitro caspase-3/7 luminescent assay was performed to determine the potency of conatumumab, DOTA-conatumumab, and copper-DOTA-conatumumab to induce caspase-3/7 activities in Colo205 tumor cells. The study results showed that the effective doses ( $ED_{50} \pm$  SD) of conatumumab and DOTA-conatumumab to induce 50% of the maximum caspase-3/7 activities in Colo205 tumor cells

were similar at  $20 \pm 4.6$  and  $19 \pm 4.4$  ng/mL, or  $135 \pm 31$  and  $128 \pm 30$  pM, respectively. The  $ED_{50}$  of copper-DOTA-conatumumab was also similar at  $25.0 \pm 7.0$  ng/mL. A reference standard of conatumumab was also tested in this assay, and the relative potency of DOTA-conatumumab and copper-DOTA-conatumumab, compared with the reference standard, was  $102.8\% \pm 11.5\%$  and  $84.8\% \pm 2.9\%$ , respectively (Table 1).

#### **In Vivo Biologic Activity of DOTA-Conatumumab**

To further confirm that DOTA-modified conatumumab maintains conatumumab-like activity, an in vivo biologic activity assay was performed. A vehicle control group and an IgG1 isotype control group were also included in the assay. The data from these studies are shown in Figure 2. At a dose of 0.25  $\mu$ g, tumor growth in all 3 treatment groups was similar to that of the vehicle controls and the IgG1 isotype controls. At a dose of 2.5  $\mu$ g, all 3 treatment groups showed tumor stasis; tumors continued to grow in the control groups. Tumor regression was observed at a dose of 25  $\mu$ g for all treatment groups.

#### **$^{64}\text{Cu}$ -DOTA-Conatumumab**

$^{64}\text{Cu}$ -DOTA-conatumumab was prepared by incubating  $^{64}\text{CuCl}_2$  with DOTA-conatumumab. Three different batches were prepared for stability, small-animal PET, and biodistribution studies. Adequate yields (26%–46%), high radiochemical purity (>95%), and high specific activity (>0.8 MBq/ $\mu$ g protein) were achieved. In addition,  $^{64}\text{Cu}$ -DOTA-conatumumab was found to be stable in mouse serum at 37°C for at least 24 h. In vivo studies in CB17 SCID mice showed that greater than 98% of blood radioactivity was attributable to  $^{64}\text{Cu}$ -DOTA-conatumumab at 1, 6, and 24 h after administration.

#### **Imaging of DR5-Positive Tumors with Small-Animal PET**

SCID mice bearing Colo205 tumors were used in small-animal PET studies. Each animal received approximately 3.7 MBq of  $^{64}\text{Cu}$ -DOTA-conatumumab with a mass of 4.5  $\mu$ g of DOTA-conatumumab. The animals in the blocking group also received a 400- $\mu$ g dose of conatumumab. Immediate qualitative analysis of the imaging data was performed at the end of the first imaging session to ensure radiopharmaceutical injection accuracy. PET images were coregistered with CT images for anatomic visualization. Representative small-animal PET images from 3 different time points (1, 6, and 24 h) and the 24-h PET/CT coregistered images are presented in Figures 3A and 3B, respectively. High levels of background radioactivity were observed at 1 and 6 h. Tumor uptake was evident by 6 h after injection. At 24 h after injection, high tumor uptake was observed in the control group, with a mean SUV of 3.16 ( $n = 2$ ). Tumor uptake was decreased substantially by the coinjection of conatumumab in the blocking group, and the mean SUV dropped to 1.55 ( $n = 2$ ), suggesting saturable uptake. The spleen also displayed saturable uptake, and the corresponding

**TABLE 1**  
ED<sub>50</sub> and Relative Potency of DOTA-Conatumumab and Copper-DOTA-Conatumumab, Compared with Conatumumab, in In Vitro Apoptosis Assay

Sample	ED <sub>50</sub>		Percentage coefficient of variation	Relative potency (mean ± SD)	n
	ng/mL ± SD	pM ± SD			
Conatumumab	20 ± 4.6	135 ± 31	23.2	100.0% ± 3.4%	5
DOTA-conatumumab	19 ± 4.4	128 ± 30	22.6	102.8% ± 11.5%	5
Copper-DOTA-conatumumab*	25.0 ± 7.0		28.0	84.8% ± 2.9%	3

\*Molecular weight cannot be accurately determined with mass spectrometry.

mean SUVs for the control and blocking groups were 1.73 and 1.23, respectively. All other tissues showed nonsaturable uptake, the liver having SUVs of 1.83 and 1.80 (2 experiments).

#### Biodistribution of <sup>64</sup>Cu-DOTA-Conatumumab

Biodistribution studies were performed to examine the whole-body distribution of the tracer. Each tumor-bearing animal received approximately 0.33 MBq of <sup>64</sup>Cu-DOTA-conatumumab (~8 µg). The blocking group also received 400 µg of conatumumab. The study results are summarized in Table 2. For the control groups, tumor uptake (%ID/g ± SD) at 6 and 24 h after injection was 13.86 ± 1.19 and 20.68 ± 3.03, respectively. Under blocking conditions, tumor uptake (±SD) at 6 and 24 h decreased to 9.70 ± 1.06 and 11.76 ± 1.74, respectively, showing that the tumor uptake of the tracer is a saturable and specific process and consistent with the small-animal PET findings.

In addition to the tumor, saturable splenic uptake was also observed. For the control group, splenic uptake (%ID/g ± SD) at 6 and 24 h after injection was 46.72 ± 5.30 and 42.66 ± 10.93, respectively. Under blocking conditions, splenic uptake decreased to 14.00 ± 1.74 and 16.15 ± 1.84, respectively.

#### Autoradiography Studies to Confirm Saturable Tumor Uptake

Autoradiography images of tumor slices from the control and blocking groups are shown in Figure 4. High uptake was observed throughout the control tumor slices. Under blocking conditions, most of the tumor uptake (especially in the center of the tumor) was blocked by the coadministration of conatumumab, leaving residual uptake only near the surface of the tissue.

#### DISCUSSION

Apoptosis may be induced in some cancers by activating the p53-independent extrinsic apoptosis pathway through activation of death receptors (5). Conatumumab is a DR5-specific agonistic antibody that binds to DR5 with high affinity, induces caspase activation in Colo205 tumor cells, and inhibits tumor growth in SCID mice bearing Colo205 xenograft tumors (6). Conatumumab is currently under investigation as a potential oncology therapeutic agent (8). In this report, we describe the synthesis and characterization of DOTA-conatumumab and <sup>64</sup>Cu-DOTA-conatumumab with the goal of using <sup>64</sup>Cu-DOTA-conatumumab as a noninva-

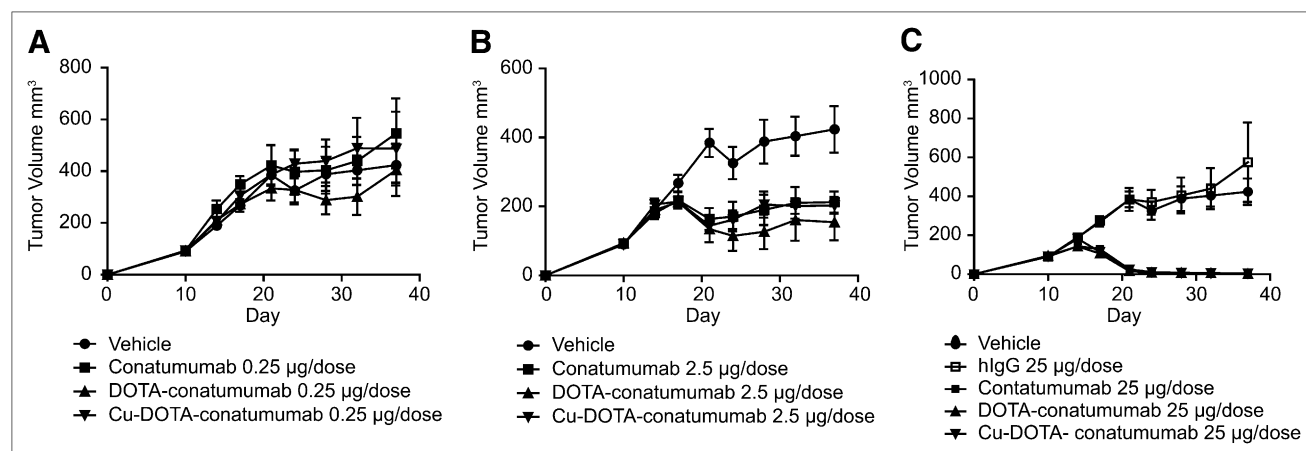


**FIGURE 2.** Treatment of SCID mice bearing human Colo205 tumor xenografts with conatumumab, DOTA-conatumumab, and copper-DOTA-conatumumab. Tumor growth inhibition after administration of DOTA-conatumumab and copper-DOTA-conatumumab at 3 dose levels was the same as that of conatumumab: 0.25 µg (A), 2.5 µg (B), and 25 µg (C).

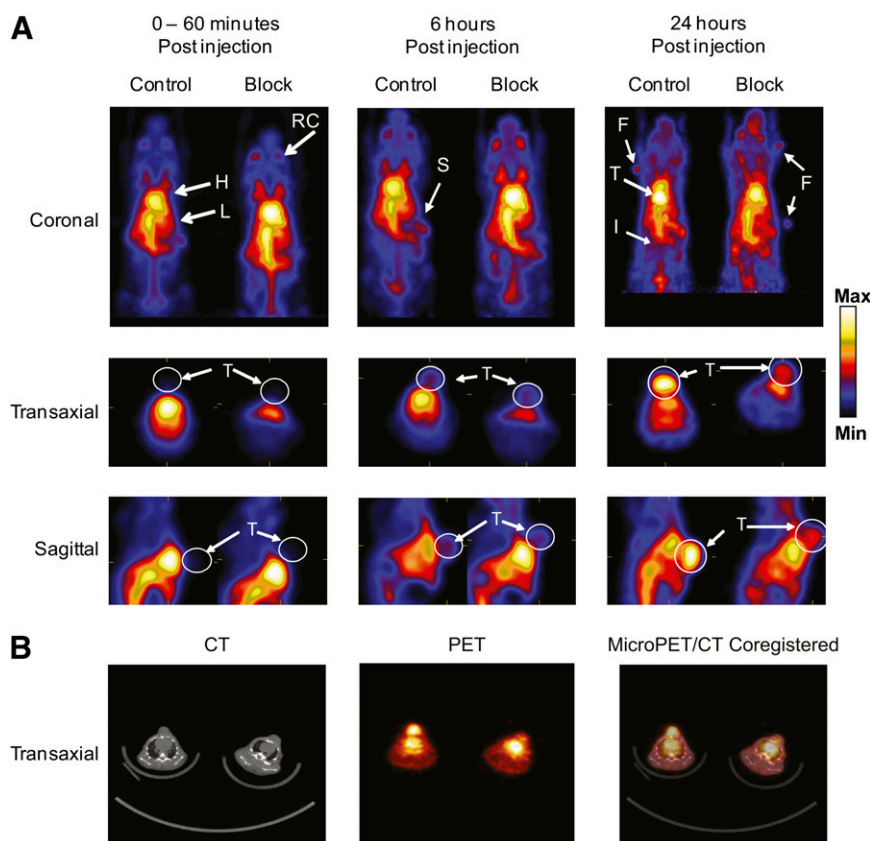


**FIGURE 3.** (A) Small-animal PET images of SCID mice bearing Colo205 tumors. (B) CT, 24-h small-animal PET, and CT/small-animal PET coregistered transaxial images of SCID mice bearing Colo205 tumors. Image on left is control animal, and image on right is block animal. F = fiducial markers (for small-animal PET/micro-CT coregistration); H = heart; I = intestine; L = liver; max = maximum; min = minimum; RC = retroorbital cavity; S = spleen; T = tumor.

sive PET tracer to inform clinical dose selection by measuring tumor DR5 receptor occupancy. This approach requires a tracer with high specific activity to ensure that the injected tracer itself does not result in significant receptor occupancy and downstream pharmacologic effects.

We demonstrated that DOTA can be efficiently coupled to conatumumab. The absolute number of DOTA molecules per conatumumab molecules measured via MS assays ( $\sim 5$

DOTA molecules per conatumumab molecule) was slightly higher than the average number determined by the isotope dilution method ( $\sim 4$  DOTA molecules per antibody). The lower number of functional chelators observed using the isotope dilution technique may have been due to the inaccessibility of some of the DOTA chelates to the copper atoms.

The *in vitro* potency of DOTA-conatumumab and copper-DOTA-conatumumab for DR5 was similar to that of

**TABLE 2**  
Biodistribution of  $^{64}\text{Cu}$ -DOTA-Conatumumab in Female SCID Mice Bearing Colo205 Tumors

Organ	Uptake of $^{64}\text{Cu}$ -DOTA-conatumumab (%ID/g $\pm$ SD)					
	6 h	6-h block	24 h	24-h block	24 h after PET*	24 h after PET block*
Blood	24.53 $\pm$ 1.76	25.10 $\pm$ 1.56	18.14 $\pm$ 1.49	18.21 $\pm$ 0.99	21.45 $\pm$ 0.68	22.02 $\pm$ 0.25
Lung	9.82 $\pm$ 0.53	9.59 $\pm$ 0.47	9.30 $\pm$ 0.53	8.98 $\pm$ 0.85	11.79 $\pm$ 0.86	11.77 $\pm$ 1.78
Liver	13.32 $\pm$ 0.58	12.17 $\pm$ 0.91	10.75 $\pm$ 1.07	8.81 $\pm$ 0.54	8.31 $\pm$ 0.81	7.21 $\pm$ 0.59
Spleen	46.72 $\pm$ 5.30	14.00 $\pm$ 1.74	42.66 $\pm$ 10.93	16.15 $\pm$ 1.84	33.10 $\pm$ 3.43	13.99 $\pm$ 0.87
Kidney	7.44 $\pm$ 0.25	8.14 $\pm$ 1.03	5.99 $\pm$ 0.83	6.03 $\pm$ 0.93	7.23 $\pm$ 0.47	7.31 $\pm$ 1.82
Muscle	2.47 $\pm$ 0.82	2.56 $\pm$ 0.07	3.20 $\pm$ 0.30	2.68 $\pm$ 0.29	5.32 $\pm$ 0.62	4.01 $\pm$ 0.25
Fat	5.70 $\pm$ 2.22	4.15 $\pm$ 0.52	3.46 $\pm$ 0.58	4.05 $\pm$ 0.96	5.37 $\pm$ 2.36	3.97 $\pm$ 1.27
Heart	7.96 $\pm$ 0.38	6.25 $\pm$ 0.49	6.06 $\pm$ 0.52	5.77 $\pm$ 0.71	7.51 $\pm$ 0.91	6.22 $\pm$ 2.49
Brain	0.70 $\pm$ 0.13	0.71 $\pm$ 0.13	0.60 $\pm$ 0.09	0.67 $\pm$ 0.10	0.76 $\pm$ 0.05	0.70 $\pm$ 0.02
Bone	5.07 $\pm$ 0.63	2.88 $\pm$ 0.26	3.74 $\pm$ 0.38	2.32 $\pm$ 0.22	3.54 $\pm$ 0.25	2.93 $\pm$ 0.07
Tumor	13.86 $\pm$ 1.19	9.70 $\pm$ 1.06	20.68 $\pm$ 3.03	11.76 $\pm$ 1.74	28.38 $\pm$ 0.74	11.20 $\pm$ 1.08

\*Coinjected with 400  $\mu\text{g}$  of conatumumab.

Data are mean %ID/g  $\pm$  SD ( $n = 4$ ). Animals ( $n = 2$ ) were sacrificed after last small-animal PET scan (24 h).

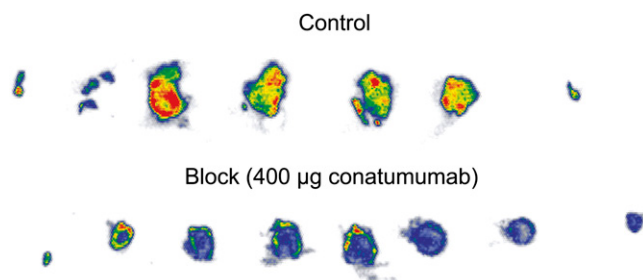


**FIGURE 4.** Autoradiography images of tumor slices from control animal and block animal. Results confirmed that tumor uptake of  $^{64}\text{Cu}$ -DOTA-conatumumab was blocked by coadministration of 400  $\mu\text{g}$  of conatumumab.

the reference standard of conatumumab. Although there were small differences observed between conatumumab, DOTA-conatumumab, and copper-DOTA-conatumumab in this assay, they are well within the established batch acceptance criteria for conatumumab. In vivo studies in Colo205 xenografts also showed that DOTA-conatumumab and copper-DOTA-conatumumab have biologic function and potency comparable to that of unmodified conatumumab, supporting the use of  $^{64}\text{Cu}$ -DOTA-conatumumab for in vivo imaging of tumors that express DR5. This use is further supported by the observation that the pharmacokinetic profiles of  $^{64}\text{Cu}$ -DOTA-conatumumab and conatumumab are similar (data to be presented in a separate report).

As expected,  $^{64}\text{Cu}$ -DOTA-conatumumab was readily prepared from DOTA-conatumumab and  $^{64}\text{CuCl}_2$ . Blood metabolite analyses, both in vitro and in vivo, showed that the tracer was stable in blood at all time points examined. Small-animal PET studies clearly demonstrated that Colo205 tumors readily take up the tracer, with a mean SUV of 3.16 by 24 h after injection. This uptake could be blocked (SUV, 1.55) by the coadministration of an excess of unlabeled conatumumab, suggesting that tumor uptake was competitively blocked and hence specific. The SUV was related to the %ID/g. An SUV of 3.16 corresponds to 17.6 %ID/g, and an SUV of 1.55 corresponds to 8.61 %ID/g. These values agree well with the biodistribution data shown in Table 2.

The biodistribution study yielded a control–block tumor uptake (%ID/g) ratio of 2.5 at 24 h after injection, which is slightly higher than the corresponding SUV ratio of 2 determined by small-animal PET. The lower SUV ratio measured by small-animal PET may have been due to spillover effects from adjacent organs containing high levels of radioactivity, a potential limitation of implanting tumors in the mid-thoracic region. These effects could lead to higher observed tumor uptake under blocking conditions. Saturable uptake was also observed in the spleen, probably because of binding of the tracer to splenic Fc receptors on macrophages. The mechanism of splenic uptake has been investigated with an Fc receptor–specific antibody and will be presented in a separate publication.

Saturable tumor uptake of  $^{64}\text{Cu}$ -DOTA-conatumumab was further confirmed by autoradiography of tumors. As

seen in Figure 4, high tumor uptake was observed under control conditions. Coinjection of conatumumab decreased tumor uptake, with radioactivity observed near the surface of the tumor, possibly because of the residual blood pool.

Radiolabeled apoptosis-inducing antibodies are often used as radioimmunotherapy agents (15). It is, therefore, feasible that conatumumab labeled with  $^{64}\text{Cu}$  or other radionuclides such as  $^{67}\text{Cu}$  or  $^{90}\text{Y}$  (16,17) could be used as a radioimmunotherapy agent.

## CONCLUSION

Our results clearly demonstrate that  $^{64}\text{Cu}$ -DOTA-conatumumab can potentially be used as an imaging tracer to detect DR5 in tumors. Additional dose–response studies and blocking studies using an Fc receptor–specific IgG would be helpful to demonstrate the applicability of this imaging technique to monitor DR5 occupancy by conatumumab.

## DISCLOSURE STATEMENT

The costs of publication of this article were defrayed in part by the payment of page charges. Therefore, and solely to indicate this fact, this article is hereby marked “advertisement” in accordance with 18 USC section 1734.

## ACKNOWLEDGMENTS

We thank the Washington University Cyclotron Facility; the microPET Imaging Facility; the Amgen conatumumab team members, Jon Graves, Jeff Wiezorek, Sylvie Tiso, and Opas Noi Nuanmanee, for their helpful discussions; and Kathryn Boorer for editorial assistance. The study was supported by Amgen Inc. Production of  $^{64}\text{Cu}$  was supported by a grant from the National Cancer Institute (CA86307). Thomas Arroll, Ching Chen, Art Hewig, Paula Kaplan-Lefko, Greg Friberg, Robert Radinsky, and Dah-Ren Hwang are employees of Amgen Inc. and own stock in Amgen Inc; Michael J. Welch has received a research grant from Amgen Inc.

## REFERENCES

1. Ashkenazi A, Dixit VM. Death receptors: signaling and modulation. *Science*. 1998;281:1305–1308.
2. Ashkenazi A. Targeting death and decoy receptors of the tumour-necrosis factor superfamily. *Nat Rev Cancer*. 2002;2:420–430.
3. Spierings DC, de Vries EG, Vellenga E, et al. Tissue distribution of the death ligand TRAIL and its receptors. *J Histochem Cytochem*. 2004;52:821–831.
4. Kelley RF, Totpal K, Lindstrom SH, et al. Receptor-selective mutants of apoptosis-inducing ligand 2/tumor necrosis factor-related apoptosis-inducing ligand reveal a greater contribution of death receptor (DR) 5 than DR4 to apoptosis signaling. *J Biol Chem*. 2005;280:2205–2212.
5. Ashkenazi A, Herbst RS. To kill a tumor cell: the potential of proapoptotic receptor agonists. *J Clin Invest*. 2008;118:1979–1990.
6. Kaplan-Lefko PJ, Graves JD, Zoog SJ, et al. Conatumumab, a fully human agonist antibody to death receptor 5, induces apoptosis via caspase activation in multiple tumor types. *Cancer Biol Ther*. 2010;9:618–631.
7. LoRusso P, Hong D, Heath E, et al. First-in-human study of AMG 655, a proapoptotic TRAIL receptor-2 agonist, in adult patients with advanced solid tumors [abstract]. *J Clin Oncol*. 2007;25(June 20 suppl):3534.
8. Wiezorek J, Holland P, Graves J. Death receptor agonists as a targeted therapy for cancer. *Clin Cancer Res*. 2010;16:1701–1708.

9. Gong J, Yang D, Kohanim S, Humphreys R, Broemeling L, Kurzrock R. Novel in vivo imaging shows up-regulation of death receptors by paclitaxel and correlates with enhanced antitumor effects of receptor agonist antibodies. *Mol Cancer Ther.* 2006;5:2991–3000.
10. McCarthy DW, Shefer RE, Klinkowstein RE, et al. Efficient production of high specific activity  $^{64}\text{Cu}$  using a biomedical cyclotron. *Nucl Med Biol.* 1997;24:35–43.
11. Tang L. Radionuclide production and yields at Washington University School of Medicine. *Q J Nucl Med Mol Imaging.* 2008;52:121–133.
12. Jensen MM, Jorgensen JT, Binderup T, Kjaer A. Tumor volume in subcutaneous mouse xenografts measured by microCT is more accurate and reproducible than determined by  $^{18}\text{F}$ -FDG-microPET or external caliper. *BMC Med Imaging.* 2008;8:16.
13. Euhus DM, Hudd C, LaRegina MC, Johnson FE. Tumor measurement in the nude mouse. *J Surg Oncol.* 1986;31:229–234.
14. Sun X, Rossin R, Turner JL, et al. An assessment of the effects of shell cross-linked nanoparticle size, core composition, and surface PEGylation on in vivo biodistribution. *Biomacromolecules.* 2005;6:2541–2554.
15. DeNardo GL, O'Donnell RT, Kroger LA, et al. Strategies for developing effective radioimmunotherapy for solid tumors. *Clin Cancer Res.* 1999;5:3219s–3223s.
16. Apelgot S, Coppey J, Gaudemer A, et al. Similar lethal effect in mammalian cells for two radioisotopes of copper with different decay schemes,  $^{64}\text{Cu}$  and  $^{67}\text{Cu}$ . *Int J Radiat Biol.* 1989;55:365–384.
17. Grunberg J, Novak-Hofer I, Honer M, et al. In vivo evaluation of  $^{177}\text{Lu}$ - and  $^{67/64}\text{Cu}$ -labeled recombinant fragments of antibody chCE7 for radioimmunotherapy and PET imaging of L1-CAM-positive tumors. *Clin Cancer Res.* 2005;11:5112–5120.





The Journal of  
NUCLEAR MEDICINE

## Characterization of $^{64}\text{Cu}$ -DOTA-Conatumumab: A PET Tracer for In Vivo Imaging of Death Receptor 5

Raffaella Rossin, Tadahiko Kohno, Aviv Hagooly, Terry Sharp, Brian Gliniak, Thomas Arroll, Qing Chen, Art Hewig, Paula Kaplan-Lefko, Greg Friberg, Robert Radinsky, Jeffrey L. Evelhoch, Michael J. Welch and Dah-Ren Hwang

*J Nucl Med.* 2011;52:942-949.

Published online: May 13, 2011.

Doi: 10.2967/jnumed.110.086157

---

This article and updated information are available at:

<http://jnm.snmjournals.org/content/52/6/942>

---

Information about reproducing figures, tables, or other portions of this article can be found online at:

<http://jnm.snmjournals.org/site/misc/permission.xhtml>

Information about subscriptions to JNM can be found at:

<http://jnm.snmjournals.org/site/subscriptions/online.xhtml>

*The Journal of Nuclear Medicine* is published monthly.  
SNMMI | Society of Nuclear Medicine and Molecular Imaging  
1850 Samuel Morse Drive, Reston, VA 20190.  
(Print ISSN: 0161-5505, Online ISSN: 2159-662X)

© Copyright 2011 SNMMI; all rights reserved.

 SOCIETY OF  
NUCLEAR MEDICINE  
AND MOLECULAR IMAGING